International Journal of Marine Engineering Innovation and Research, Vol. 10(1), March. 2025. 1-11
(pISSN: 2541-5972, eISSN: 2548-1479)

Study and Analysis of the Performance of the Propulsion System of the K-61 Type Amphibious Vehicle for Artillery Transport (KAPA)

Good Rindo[1], Ahmad Fauzan Zakki[2], Farell Elghifari Putratama[3], Berlian Arswendo Adietya[4] ,Sapto Wiratno Satoto[5]

(Received: 23 November 2024 / Revised: 03 December 2024 /Accepted: 05 January 2025 / Available Online: 21 March 2025)

Abstract– The application of waterjet propulsion systems in amphibious combat vehicles, such as the KAPA Type K-61 used by the Indonesian National Armed Forces (TNI) for transporting artillery munitions, is crucial for enhancing operational performance. The working principle of a waterjet involves drawing water from beneath the vehicle's hull, accelerating it through a pump, and expelling it to generate thrust. The design of the waterjet propulsion system significantly impacts the thrust produced. This study aims to evaluate the maximum performance achievable by the waterjet propulsion system of the KAPA Type K-61. The analysis is conducted using various Index Velocity Ratio (IVR) values, including IVR 0.28, which represents the current speed of the KAPA Type K-61, and other variations such as IVR 0.54, 0.59, 0.67, 0.70, 0.78, 0.94, 1.18, 1.64, and 2.38. The analysis results include the thrust value produced at the waterjet outlet, efficiency, and propulsion power. The study found that at an IVR of 2.38, the system produced the highest thrust of 30.72 N, with a propulsion power of 7315.13 Watts, equivalent to 9.95 Horsepower, and the highest efficiency of 99.21%. Based on the research conducted, it is recommended that future studies create a geometric model of the KAPA Type K-61 with original and more detailed dimensions and perform a 1:1 scale analysis to strengthen the obtained results. Additionally, analyzing the waterjet propulsion system along with the impeller or propeller system is also suggested to gain a more comprehensive understanding of the overall propulsion system's performance and efficiency.

Keywords— *Propulsion system, index velocity ratio (IVR), Amphibious Vehicle for Artillery Transport KAPA, Effiency, Thrust*

I. INTRODUCTION

In supporting operational execution, the Indonesian National Armed Forces (TNI) will use various equipment to ensure the success of these operations, including the use of amphibious vehicles (1). In the field of defense, there are various technologies focusing on different aspects, particularly in terms of security and military superiority. One such technology is the Amphibious Artillery Carrier Vehicle (KAPA) Type K-61 (2).

To enhance the operational capability of the Amphibious Armored Personnel Carrier (AAPC) through the characteristics of its propulsion system, visualization tests of the underwater flow are conducted. This research is carried out by observing the fluid flow around the lower and rear parts of the vehicle, including the intake section of the propulsion system (3). Waterjet propulsion is widely used in various types of maritime vessels, such as high-speed ferries, yachts, and amphibious vehicles. In this context, the propulsion system used in the KAPA Type K-61 applies waterjet propulsion for water operation (4). The waterjet propulsion system is widely used in both civilian and military applications due to its high system efficiency, strong anti-cavitation capabilities, excellent maneuverability, stable operational performance, and relatively low noise levels (5).

The waterjet propulsion system operates by drawing water from the bottom of the ship's hull and then pushing it through the pressure of a pump from a turbine, ejecting it through the rear (outlet) to generate thrust for the vehicle (6). Water is sprayed from the outlet/nozzle with the aid of the pump thrust in the waterjet, which draws water from the bottom of the vehicle (7). The distribution of water flow through the pump and the outlet via the nozzle is influenced by the vehicle's intake section (8).

An analysis conducted on a waterjet inlet model installed on the sidewall of a wind tunnel has found that there is a separation zone at the roof of the flow duct, and the outcome is highly dependent on the Reynolds number (9). Differences in the flow at the outlet, whether uniform or non-uniform suction flow, have become a significant concern. Previous studies have confirmed that

Good Rindo Department of Naval Architecture Diponegoro University, Semarang, 50275. E-mail: good.rindo@gmail.com
Ahmad Fauzan Zakki[1] Department of Naval Architecture Diponegoro University, Semarang, 50275. E-mail: ahmadfzakki@yahoo.com
Farell Elghifari Putratama Department of Naval Architecture Diponegoro University, Semarang, 50275. E-mail: farellelghifari@alumni.undip.ac.id
Berlian Arswendo Adietya Department of Naval Architecture Diponegoro University, Semarang, 50275. E-mail: berlianarswendokapal@gmail.com
Sapto Wiranto Satoto, Department of ship construction polytechnic, batam, 50275. E-mail: sapto@polibatam.ac.id

uneven suction flow can cause a significant reduction in pump performance, indicated by noticeable vortex distortion at the top and the formation of circular vortices (10). This suggests that suction flow consistency is a critical factor to consider in maintaining the efficiency and performance of the pump system (11).

The ITTC Specialist Committee on Waterjets has formulated research procedures to investigate interactions in waterjet experiments through step-by-step procedures that include precise measurements, the use of advanced instruments, and in-depth data analysis. The goal is to understand how waterjets interact with their environment, such as their use as ship propulsion or their application in industrial fields, and to gain a better understanding of the dynamics of waterjets along with potential technological developments (12).

Results from other experimental studies also show that the relationship between the waterjet flow and the hull was tested using several experiments with both scaled model dimensions and models with original dimensions. The findings from these studies reveal several potential factors that impact the overall interaction and recognize the magnitude of the waterjet's momentum induced by lift forces and moments at the center of gravity (13).

The development of waterjet propulsion technology continues to advance rapidly. Many researchers have utilized Computational Fluid Dynamics (CFD) methods to conduct numerical simulations of waterjet propulsion systems (14). The goal is to study the interaction between the waterjet propeller and the hull as an integral part of the overall waterjet propulsion system design process (15). A methodology is also presented for verifying and validating the CFD simulation results of a RANS CFD code developed for specific purposes, specific geometries, specific conditions, and available benchmark information. Concepts and definitions are provided to improve errors and uncertainties, as well as the simulation verification and validation processes (16).

Research focusing on the performance effects of waterjet pumps has provided evidence that the slower the pump's rotational speed, the less thrust generated by the propulsion system (17). An analysis of high-pressure waterjet propulsion with a pressure vector control system applied to underwater vehicles provides a detailed overview of a system with control capabilities that effectively suppresses overshoot values and shows significant improvements in stability (18).

This study utilizes the Variation Index Velocity Ratio (IVR) to analyze the propulsion system's performance, identifying the conditions under which maximum efficiency is achieved. Optimizing the IVR value minimizes resistance, enhances efficiency, and improves vessel stability, ultimately leading to a substantial improvement in the vessel's overall operational performance.

II. METHOD

A. Research Methodology

This research began with a literature review, followed by the collection of primary and secondary data on the research object, namely the KAPA Type K-61, variations in the Index Velocity Ratio (IVR) values, and vehicle speed. Next, a 3D model was designed based on previous research as a reference, followed by a CFD simulation analysis, and finally, verification and validation of the obtained data. This research method is based on the existing problem formulation, derived from literature and theoretical understanding related to the issue. Data validity is given significant attention, with testing based on CFD. The research analysis results include the performance analysis of the KAPA Type K-61 waterjet propulsion system, presented in the form of conclusions and recommendations for the development of future research.

B. Research Object

The object of the research is the waterjet propulsion system of the Amphibious Artillery Carrier Vehicle (KAPA) Type K-61 (Figure 1.), with the following vehicle specifications :

- Length : 9.15 m
- Width : 3.15 m
- Height : 2.15 m
- Displacement : 9,550 kg
- Engine : Diesel YaAz-M204VKr 4-Cylinder Water-cooled 135 Hp at 2000 rpm
- Speed : 10 km/h (in water) / 36 km/h (on land)
- Range : 260 km / 140.4 Nautical Miles

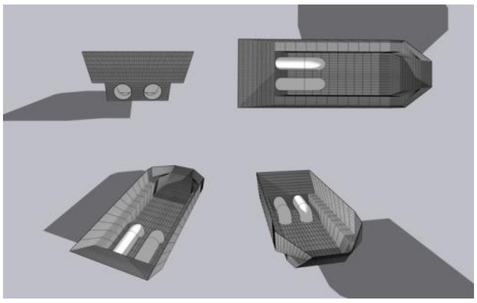

Figure 1. KAPA (Amphibious Artillery Carrier Vehicle) Type K-61.

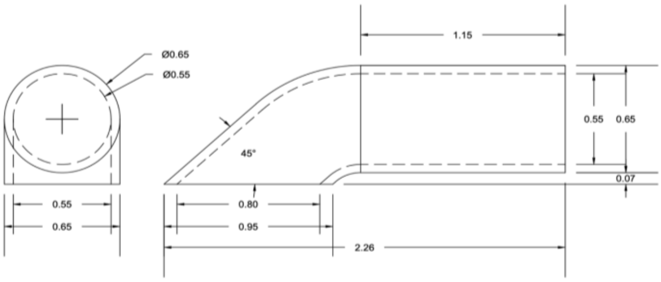

Figure 2. KAPA (Amphibious Artillery Carrier Vehicle) Type K-61

Figure 3. KAPA (Amphibious Artillery Carrier Vehicle) Type K-61.

C. Waterjet Geometry

The dimensions of the waterjet propulsion system for the KAPA Type K-61 were obtained through a tracing method based on the limited available information. It was found that the inlet (outlet) diameter is 650 mm, with an overall length of 2260 mm. The front tube section has a length of 1150 mm, the inlet length is 950 mm, and the outlet height from the baseline is 70 mm (Figure 2.). After obtaining these dimensions, a 3D model (Figure 3.) was created using a 1:10 scale of the original size. This scale is based on previous research with a similar model.

D. Boundary Condition

In this simulation, the computation is divided into two parts, the waterjet model and the fluid domain (Figure 4). The dimensions of the domain are determined with a length of 30 x Do, width of 10 x Do, height of 8 x Do, and the distance from the waterjet model inlet to the domain inlet is 25 x Do, where (Do) represents the diameter of the waterjet outlet. In this study, the reference speed used for the KAPA Type K-61 is set at 10 m/s, and the fluid density used is seawater.

The me shing stage in Computational Fluid Dynamics (CFD) is one of the critical steps in the fluid flow simulation process. At this stage, the continuous fluid domain is divided into discrete elements or cells that form the computational grid. In this simulation, the meshing strategy applied uses a maximum size of 15 mm on the waterjet model, while the entire fluid domain has a size of 200 mm. The type of mesh used is hexahedral, which offers advantages in providing high resolution and computational efficiency. With this mesh setup, the simulation results can provide better detail in specific areas, such as the waterjet model, while maintaining efficient

E. Reynolds-Averaged Navier-Stokes Equations for Turbulence Modeling

Turbulence modeling involves formulating partial differential equations to calculate turbulent flow, based on the approximation of the Navier-Stokes equations. In the Reynolds-averaged Navier-Stokes (RANS) approach, flow variables are decomposed into mean and fluctuating components, followed by their substitution into the Navier-Stokes equations and averaging to produce the Reynolds stress tensor (19). The closure problem of the Navier-Stokes system of equations consists of this

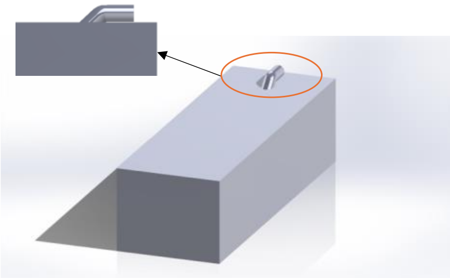

Figure 4. Domain Shape and Waterjet Model Position.

operation. The RANS equations used in this analysis consist of the continuity equation (1), momentum equation (2), and energy equation (3). These equations conserve mass, regulate momentum changes, and describe energy changes in the fluid flow (20,21). The equations are presented sequentially as follows :

$$\frac{D_\rho}{D_t} + \rho \frac{\partial U_i}{\partial x_i} = 0 \quad (1)$$

$$\rho \frac{\partial U_j}{\partial_t} + \rho U_i \frac{\partial U_j}{\partial x_t} = \frac{\partial P}{\partial x_j} - \frac{\partial \tau_{ij}}{\partial x_i} + \rho g_j \quad (2)$$

$$\rho c_\mu \frac{\partial T}{\partial_t} + \rho c_\mu U_i \frac{\partial T}{\partial x_i} = -P \frac{\partial U_i}{\partial x_t} + \lambda \frac{\partial^2 T}{\partial x_i^2} + \tau_{ij} \frac{\partial U_j}{\partial x_i}, \quad (3)$$

F. Index Velocity Ratio

Flow velocity plays an important role in explaining the flow phenomena at the inlet during the transition from ship speed to pump speed, affecting the flow characteristics and propulsion system efficiency. The ITTC has identified two important coefficients: the Jet Velocity Ratio (JVR) and the Inlet Velocity Ratio (IVR). IVR, in particular, is used to describe the flow conditions within the intake duct, which determines the efficiency of the flow in generating thrust by the pump. In waterjet propulsion system design, a proper understanding of IVR allows for the optimization of intake duct configurations to enhance overall performance and propulsion system efficiency (22). The formulas for calculating water discharge (4), inlet flow velocity (5), and IVR (6) are outlined as follows :

$$Q = A \; x \; V_j \quad (4)$$

$$V_j = \frac{Q}{\frac{\pi}{4} D.inlet^2} \quad (5)$$

$$IVR = \frac{V_{passage}}{V_{ship}} \quad (6)$$

Where :

Q = Water discharge (m^3/s)

A = Cross-sectional area of the duct (m^2)

V_i = Inlet flow velocity (m/s)

g. Index Velocity Ratio

Thrust in a waterjet propulsion system is generated based on Newton's third law of action-reaction. Water is drawn from the intake duct beneath the ship's hull and flows through an impeller to increase the water's pressure and velocity. The high-velocity water is then directed by guide vanes and expelled through the tail nozzle, producing a reaction force that propels the ship forward. The efficiency of the waterjet propulsion system depends on its ability to minimize energy losses and optimize the conversion of input energy into thrust. Waterjet propulsion is known for its high efficiency, particularly at high speeds, as it can accelerate a large volume of water with relatively low energy consumption [5]. The formulas for calculating thrust (7) and efficiency (8) are outlined as follows :

$$T = \rho \; x \; Q \; x \; (V_i - V_j) \quad (7)$$

$$\eta = \frac{\rho \; x \; Q \; x \; (V_i - V_j) \, V_j}{\rho \; x \; Q \; x \; (V_i - V_j) \, V_j + \frac{1}{2} \rho \; x \; Q \; (V_i - V_j)^2} \quad (8)$$

where :

T = Thrust value (N)

η = Efficiency value (%)

ρ = Water density

V_i = Outlet flow velocity (m/s)

V_j = Inlet flow velocity (m/s)

h. Propulsion Power

Propulsion power (P_T) is a measure of the power required to drive a vehicle through water using a propulsion system. In the context of a waterjet propulsion system, propulsion power encompasses the total power needed to generate sufficient thrust for the vehicle to move at a certain speed. Determining propulsion power involves several key variables, including thrust, system efficiency, and the flow velocities of water at the inlet and outlet (23). The basic formula for calculating propulsion power (9) typically refers to the principles of energy and momentum conservation in fluids, which can generally be expressed as follows :

$$P_T = \rho \; x \; Q \; x \; V_j \; x \; (V_i - V_j) \quad (9)$$

where :

P_T = Propulsion power

g. Model Verification anad Validation

1) In CFD, mesh structure is crucial for mapping the fluid domain and solving flow equations. A high-density mesh is recommended because it can capture more detail and produce more reliable and accurate simulation results. Finer meshes allow for more precise simulation of complex physical phenomena in fluids (24). Grid independence testing is essential to ensure accurate and reliable simulation results in CFD analysis. This test aims to find the optimal mesh density that provides consistent results without significantly increasing computation time. By balancing mesh density and computation time, efficiency and optimization in CFD analysis can be achieved, resulting in more effective and efficient simulations (25).

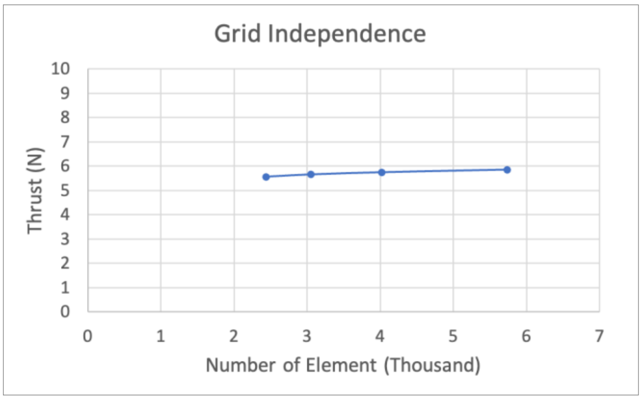

Figure 5. Graph of Mesh Element by Thrust Value.

TABLE 1.
GRID INDEPENDENCE OF THE KAPA TYPE K-61 WATERJET MODEL.

Number of Elements	57312	40242	30504	24348
Thrust (N)	5,86	5,75	5,66	5,57
Percentage (%)	-	1,9%	1,6%	1,7%

The grid independence test for the KAPA Type K-61 model (Figure 5) shows that the error level is below 2% (Table 1). This indicates that the model has good consistency and the resulting simulations are reliable with a high degree of accuracy.

2) *Thrust Validation*, In validating the thrust values, the recreated model analysis was compared with the thrust values from previous studies. The average error is 2.11%, with the lowest error at 0.29% for an IVR of 0.94 and the highest at 4.98% for an IVR of 2.38. These results are sufficient to validate the model, as the error value should not exceed 5%. With the average error below the established threshold, this validation shows that the developed model can replicate experimental results with high accuracy. Visualization and presentation of the validation data are provided in (Table 2) and visualized in (Figure 6).

3) *Output Velocity Validation*, in this section,

TABLE 2.
ERROR DATA FROM COMPARING VALIDATED THRUST RESULTS WITH PREVIOUS RESEARCH.

Validation Error			
IVR	*Thrust* (N)		*Error Rate*
	Exp. Journal	*Validation*	
0,54	14,72	14,23	3,32%
0,59	16,21	15,75	2,80%
0,67	18,58	18,25	1,79%
0,70	19,28	19,36	0,42%
0,78	21,82	21,71	0,52%
0,94	26,74	26,66	0,29%
1,18	33,93	33,10	2,44%
1,64	45,08	43,97	2,45%
2,38	59,29	56,34	4,98%
	Average		2,11%

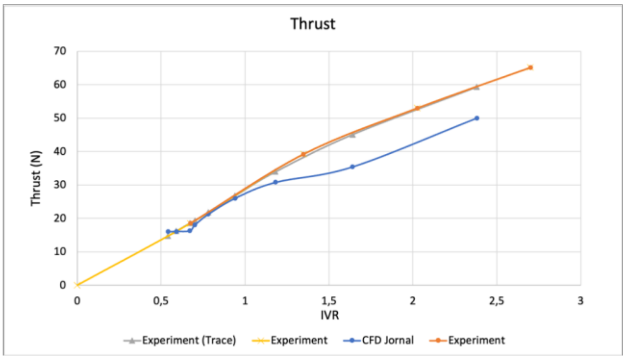

Figure 6. Graph Comparing Validated Thrust Results with Previous Research.

validation was performed on the outlet velocity results from the recreated model analysis compared with previous research results. The average error is 0.27%, with the lowest error at 0.04% for an IVR of 0.94 and the highest at 0.67% for an IVR of 0.54. These results are very good for validating the velocity component, as the error values are well below the established threshold of 5%. With such low errors, he validation indicates that the model can replicate the low velocity at the outlet with high accuracy, providing confidence that this simulation can be used for further analysis with reliable results. The validated outlet velocity data are presented in (Table 3).

4) *Efficiency Validation*, The author conducted a final validation on the efficiency values. In this section, the efficiency values from the model analysis were compared with data from previous research. The average efficiency error is 0.14%, with the lowest error at 0.02% for an IVR of 0.94 and the highest at 0.38% for an IVR of 0.54. These results are considered very good, as the error values are well below the maximum threshold of 5%. This validation indicates that the model can produce efficiency values close to experimental results, making it reliable for further analysis. The validated data are presented in (Table 4) and visualized in (Figure 7).

TABLE 3.
ERROR DATA FROM COMPARING VALIDATED OUTLET VELOCITY RESULTS WITH PREVIOUS RESEARCH.

Validation Error			
IVR	*Velocity* (m/s)		***Error Rate***
	Exp. Journal	***Validation***	
0,54	6,72	6,67	0,67%
0,59	7,25	7,21	0,53%
0,67	8,05	8,03	0,31%
0,70	8,37	8,37	0,07%
0,78	9,15	9,14	0,08%
0,94	10,77	10,77	0,04%
1,18	13,19	13,16	0,27%
1,64	17,76	17,72	0,19%
2,38	25,05	24,98	0,25%
	Average		**0,27%**

TABLE 4.
ERROR DATA FROM COMPARING VALIDATED EFFICIENCY RESULTS WITH PREVIOUS RESEARCH.

Validation Error			
IVR	*Efficiency* (%)		***Error Rate***
	Exp. Journal	***Validation***	
0,54	88,68%	89,02%	0,38%
0,59	89,58%	89,84%	0,29%
0,67	90,61%	90,76%	0,17%
0,70	91,10%	91,07%	0,04%
0,78	91,73%	91,77%	0,04%
0,94	92,94%	92,96%	0,02%
1,18	94,26%	94,39%	0,14%
1,64	96,00%	96,10%	0,10%
2,38	97,47%	97,59%	0,13%
	Average		**0,14%**

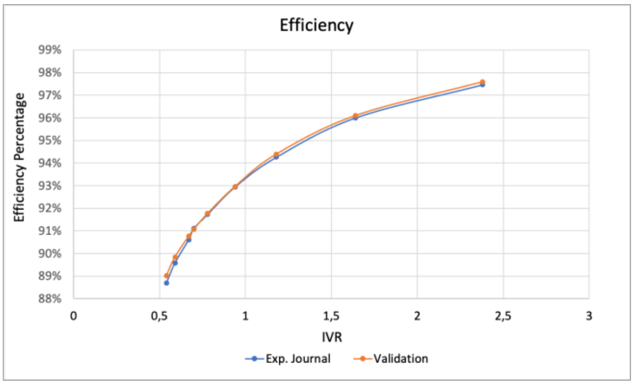

Figure 7. Graph Comparing Validated Efficiency Results with Previous Research.

III. Results and Discussion

A. Thrust Performance of KAPA Type K-61 Propulsion System

The analysis results of this study with varying IVR values for KAPA Type K-61 propulsion system model show a linear pattern, where the thrust value increases with the rising IVR or velocity ratio (Table 5). This is consistent with the results from previous research that reported the same finding. In this study, at an IVR of 0.28, which corresponds to the operational speed in water of the KAPA Type K-61, i.e., 10 km/h, the smallest thrust value of 5.86 N was produced. The results indicate that a higher IVR or velocity ratio leads to a greater thrust value. The highest thrust value was achieved at the highest IVR of 2.38, with a thrust of 30.72 N. This linear pattern (Figure 8) reinforces the finding that the design and configuration of the waterjet propulsion system have a direct correlation with the performance achieved, suggesting that adjustments to the IVR can be relied upon to improve efficiency and thrust for amphibious combat vehicles like the KAPA Type K-61.

B. Efficiency of KAPA Type K-61 Propulsion System

The analysis of KAPA Type K-61 waterjet propulsion system shows that at the current operational speed, with an IVR value of 0.28, an efficiency of 89.97% is achieved. This figure already indicates good efficiency. The study finds that higher efficiency values are achievable for the KAPA Type K-61 waterjet propulsion system.
Further analysis was conducted at different IVR values, and the results indicate that the highest efficiency is reached at an IVR of 2.38, achieving an efficiency of 99.21% (Table 6). This finding suggests that by increasing the operational speed to a higher IVR, such as 2.38, the propulsion system's efficiency can be significantly improved.

TABLE 5.
DATA FROM THRUST ANALYSIS OF KAPA TYPE K-61 WATERJET PROPULSION SYSTEM.

Thrust		
IVR	***V.Passage***	***Thrust***
0,28	2,78	5,86
0,54	5,35	9,53
0,59	5,88	10,01
0,67	6,67	10,14
0,70	7,00	10,29
0,78	7,75	10,54
0,94	9,35	11,45
1,18	11,76	12,28
1,64	16,39	15,35
2,38	23,81	30,72

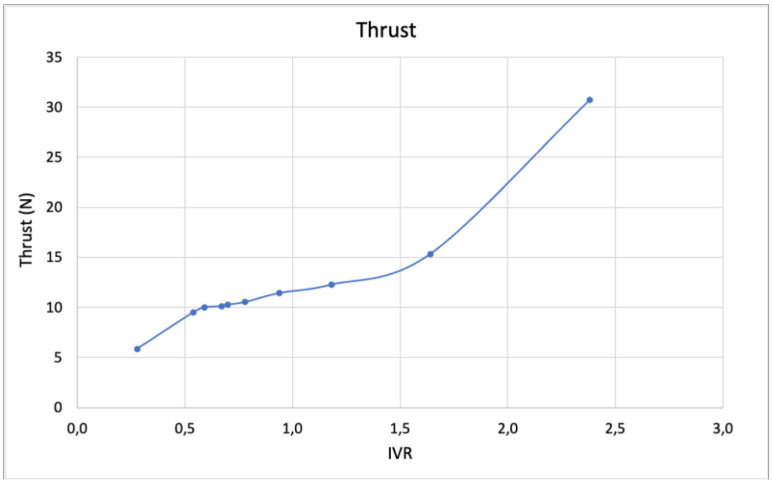

Figure 8. Graph of Thrust by IVR Value.

TABLE 6.
DATA FROM EFFICIENCY ANALYSIS OF KAPA TYPE K-61 WATERJET PROPULSION SYSTEM.

	Efficiency	
IVR	***V.Passage***	***Percentage***
0,28	2,78	89,97%
0,54	5,35	95,34%
0,59	5,88	95,92%
0,67	6,67	96,76%
0,70	7,00	97,01%
0,78	7,75	97,49%
0,94	9,35	98,11%
1,18	11,76	98,71%
1,64	16,39	99,17%
2,38	23,81	99,21%
	Thrust	
IVR	***V.Passage***	***Thrust***
0,28	2,78	5,86
0,54	5,35	9,53
0,59	5,88	10,01
0,67	6,67	10,14
0,70	7,00	10,29
0,78	7,75	10,54
0,94	9,35	11,45
1,18	11,76	12,28
1,64	16,39	15,35
2,38	23,81	30,72

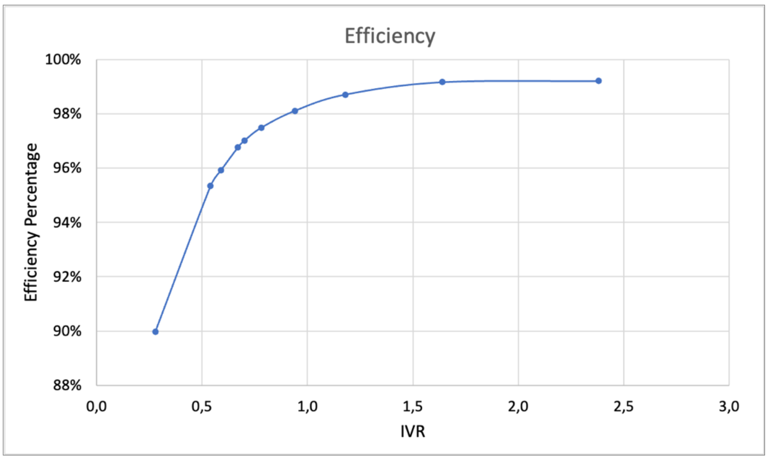

Figure 9. Graph of Efficiency by IVR Value.

The increase in efficiency with rising IVR values in the KAPA Type K-61 waterjet propulsion system model aligns with previous research findings, which demonstrate a positive relationship between IVR and propulsion system efficiency (Figure 9). A higher IVR reflects an increase in the relative speed between the water flow and the propulsion, which can enhance the generated thrust and energy conversion efficiency.

Therefore, optimizing the IVR value becomes an effective strategy to enhance the overall efficiency of the waterjet propulsion system.

C. Analysis of Propulsion Power Requirements

The analysis of the propulsion system of KAPA Type K-61 reveals that the power required to reach its operational speed is 162.77 watts, equivalent to 0.22 horsepower (Table 7). However, to achieve the speed at its potential maximum efficiency, a power of 7,315.13 watts, or 9.95 horsepower, is needed. This indicates that higher speeds require proportional propulsion power. To enhance propulsion power, certain measures can be taken.

One approach is to improve the efficiency of the engine or the propulsion system itself, such as optimizing the propeller design or improving the fuel delivery system to provide better performance. Additionally, increasing power can be achieved by using a larger engine, employing a reduction gear to provide greater torque to the propeller, or incorporating more advanced technology to generate the necessary power. All these efforts aim to ensure that sufficient power is available to reach the desired speed with optimal efficiency.

D. Analysis of Velocity Distribution at The Outlet

The results of the simulations demonstrate that altering the inlet speed or changing the IVR value results in a linear change in the velocity distribution at the outlet (Figure 10). Each variation in IVR value produces a different velocity distribution at the outlet. This finding

TABLE 7.
DATA FROM PROPULSION POWER ANALYSIS OF KAPA TYPE K-61 WATERJET PROPULSION SYSTEM.

Power			
IVR	**V.*passage***	***Propulsion Power* 1:10**	**HP 1:10**
0,28	2,78	162,77	0,22
0,54	5,35	510,06	0,69
0,59	5,88	588,59	0,80
0,67	6,67	676,04	0,92
0,70	7,00	720,42	0,98
0,78	7,75	816,95	1,11
0,94	9,35	1070,48	1,46
1,18	11,76	1444,55	1,96
1,64	16,39	2515,10	3,42
2,38	23,81	7315,13	9,95

TABLE 8.
DATA FROM THE ANALYSIS OF OUTLET VELOCITY DISTRIBUTION OF KAPA TYPE K-61 WATERJET PROPULSION SYSTEM.

Velocity		
IVR	**V.*Passage***	**V.*Outlet***
0,28	2,78	3,40
0,54	5,35	5,87
0,59	5,88	6,38
0,67	6,67	7,12
0,70	7,00	7,43
0,78	7,75	8,15
0,94	9,35	9,71
1,18	11,76	12,07
1,64	16,39	16,67
2,38	23,81	24,19

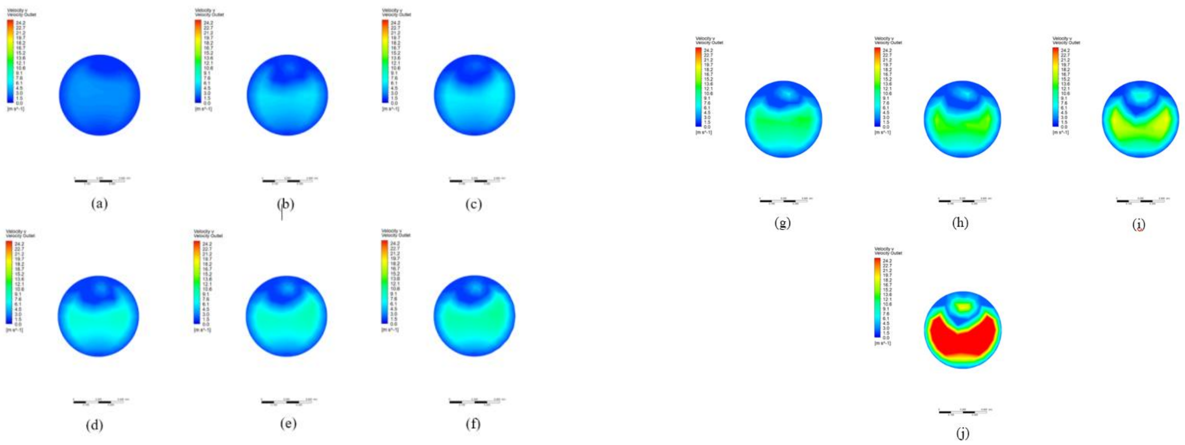

Figure 10. Velocity Distribution Contours at The Outlet by : (a) IVR 0.28, (b) IVR 0.54, (c) IVR 0.59, (d) IVR 0.67, (e) IVR 0.70, (f) IVR 0.78, (g) IVR 0.94, (h) IVR 1.18, (i) IVR 1.64, dan (j) IVR 2.38.

underscores that the IVR value directly affects the velocity distribution at the outlet, leading to varying flow characteristics at each IVR value. Additionally, it was observed that higher IVR values correspond to higher velocities at the outlet. Thus, a proportional increase in IVR results in an expanded velocity distribution area at the outlet, while areas with lower velocities tend to decrease. These findings are consistent with previous research, which shows that the IVR value plays a crucial role in regulating velocity distribution in the propulsion system and also confirms that increasing the IVR value can enhance the overall outlet flow velocity (Table 8).

IV. CONCLUSION

The analysis results from the 1:10 scale model of the KAPA Type K-61 waterjet propulsion system show that the best performance is achieved at an IVR value of 2.38, with a thrust of 30.72 N and efficiency reaching 99.21%. Despite the current operational speed, represented by an IVR value of 0.28, this propulsion system shows an efficiency of 89.97% with a thrust of 5.86 N. The analysis indicates that there is still room for further performance improvement. This aligns with findings from previous research, which suggest that as the IVR increases, both the thrust and efficiency improve.

Further analysis at various IVR values shows that shifting the operational speed of the KAPA Type K-61 waterjet propulsion to higher IVR values, such as IVR 2.38, can significantly enhance efficiency. This increased efficiency is consistent with previous research findings, which consistently show that higher IVR values reflect an increased relative speed between the water flow and propulsion, ultimately leading to greater thrust and better energy conversion efficiency. This also emphasizes the contribution of optimized waterjet propulsion systems to environmental sustainability by improving energy conversion efficiency, which in turn reduces fuel consumption and the carbon footprint of the vessel—aligned with the objectives of environmental sustainability as outlined in the scope of IOP Earth & Environmental Science.

Under the maximum performance condition based on the highest IVR value from the 1:10 scale model of the KAPA Type K-61 waterjet propulsion system, the propulsion power reaches 7315.13 watts, equivalent to 9.95 horsepower. This figure represents the power required to achieve such speed. With an average validation error of 2.11% for thrust, 0.27% for outlet velocity, and 1.02% for efficiency, the developed model is capable of replicating experimental results with high accuracy. These findings provide a clear understanding of the power required to achieve maximum performance, supporting efforts to optimize the propulsion system for more efficient and effective performance.

Based on the research and analysis conducted, several recommendations for future studies are proposed. First, it is suggested to create a more detailed full-scale geometric model to accurately interpret the characteristics of the KAPA Type K-61 propulsion system. Second, it is important to develop a 1:1 scale model and conduct experiments to reinforce the obtained results and provide more relevant data for validating simulation outcomes. Third, an analysis of the waterjet propulsion system in the KAPA Type K-61, including its impeller or propeller system, is also necessary to understand the overall performance and efficiency of the propulsion system more comprehensively. The integration of such detailed analyses would not only optimize the system's performance but also contribute further to environmental sustainability by maximizing propulsion efficiency and minimizing fuel consumption.

ACKNOWLEDGEMENTS

Thank you to the facilities provided by the Ship Design and Digitalization Laboratory at Diponegoro University, which have greatly contributed to the completion of this research.

REFERENCES

[1] Suwandi A, Purwantoro SA, Amperiawan G, Aritonang S. Kajian Teramekanika Pendaratan Kendaraan Amphibious Rig M3 Pada Tepian Sungai Terjal Dan Jenis Lempung Melalui Studi Kasus Latihan Di Gedebage Bandung Terramechanical Study of Amphibious Rig M3 Vehicle Landing on Steep Riverbanks and Clay Types Through a . J Teknol Daya Gerak [Internet]. 2022;5(1):18–30. Available from: https://www.gdels.com/m3.php

[2] Neviana O, Satrya C. Desain structure chassis kapal di aplikasikan pada chassis KAPA (kendaraan Amfibi Pengangkut Arteleri) SHIP DESIGN CHASSIS STRUCTURE IS APPLIED ON THE CHASSIS KAPA (KENDARAAN AMFIBI PENGANGKUT ARTELERI). 2016;

[3] Helvacioglu S, Helvacioglu IH, Tuncer B. Improving the river crossing capability of an amphibious vehicle. Ocean Eng [Internet]. 2011;38(17–18):2201–7. Available from: http://dx.doi.org/10.1016/j.oceaneng.2011.10.001

[4] Gong J, Wu Z, Ding J, Jiang J, Zhang Z. Numerical analysis of propulsion performance of a waterjet-propelled vehicle in steady drift. Ocean Eng [Internet]. 2022;266(P4):113136. Available from: https://doi.org/10.1016/j.oceaneng.2022.113136

[5] T. Katsoulis, X. Wang, and P. D. Kaklis, "A ..T-splines-based.. parametric.. modeller.. for.. computer..-aided.. ship design," *Ocean Engineering*, vol. 191, Nov. 2019, doi: 10.1016/j.oceaneng.2019.106433.

[6] Jiao W, Cheng L, Zhang D, Zhang B, Su Y, Wang C. Optimal Design of Inlet Passage for Waterjet Propulsion System Based on Flow and Geometric Parameters. Adv Mater Sci Eng. 2019;2019.

[7] Jiang J, Ding J, Lyu N, Luo H, Li L. Control volume determination for submerged waterjet system in self-propulsion. Ocean Eng [Internet]. 2022;265(April):112594. Available from: https://doi.org/10.1016/j.oceaneng.2022.112594

[8] Fujisawa N. Measurements of Basic Performances for Waterjet Propulsion Systems in Water Tunnel. Int J Rotating Mach. 1995;2(1):43–50.

[9] Budiyanto MA, Ayuningtyas H. PERFORMANCE ANALYSIS of WATERJET PROPULSION on AN UNMANNED SURFACE VEHICLE MODEL. J Appl Eng Sci. 2021;19(4):886–95.

[10] Roberts L. Statement of originality. Prot Promot Client Rights. 2021;(February 1998):xiii.

[11] Cao P, Wang Y, Kang C, Li G, Zhang X. Investigation of the role of non-uniform suction flow in the performance of water-jet pump. Ocean Eng [Internet]. 2017;140(March 2016):258–69. Available from: http://dx.doi.org/10.1016/j.oceaneng.2017.05.034

[12] Van Esch BPM, Bulten NWH. Numerical and experimental investigation of hydrodynamic forces due to non-uniform suction flow to a mixed-flow pump. Proc 2005 ASME Fluids Eng Div Summer Meet FEDSM2005. 2005;2005:1236–42.
[13] Van Terwisga T, Ranocchia D, Hoyt JG, Aartojarvi R, Chun HHC, Semionycheva E, et al. Report of the Specialist Committee on Validation of Waterjet Test Procedures. 24th ITTC. 2005;II.
[14] Coop HG. Investigation of hull-waterjet interaction effects. 1995;
[15] Guo J, Chen Z, Dai Y. Numerical study on self-propulsion of a waterjet propelled trimaran. Ocean Eng [Internet]. 2020;195(October 2019):106655. Available from: https://doi.org/10.1016/j.oceaneng.2019.106655
[16] Zhang L, Zhang JN, Shang YC, Dong GX, Chen WM. A Practical approach to the assessment of waterjet propulsion performance: The case of a waterjet-propelled trimaran. Polish Marit Res. 2020;26(4):27–38.
[17] Stern F, Wilson R V, Coleman HW, Paterson EG, N--- G, N--- G, et al. Verification and validation of CFD simulations. 1999;(407).
[18] Han W, Shang T, Su M, Gong C, Li R, Meng B. Direct sailing variable acceleration dynamics characteristics of water-jet propulsion with a screw mixed-flow pump. Appl Sci. 2019;9(19).
[19] Zhang Z, Cao S, Shi W, Luo X, Wang H, Deng J, et al. High pressure waterjet propulsion with thrust vector control system applied on underwater vehicles. Ocean Eng [Internet]. 2018;156(March):456–67. Available from: https://doi.org/10.1016/j.oceaneng.2018.03.009
[20] © ANSYS rights reserved. Ansys Fluent: Fluid Simulation Software. 2020 [cited 2024 Feb 1]. Available from: https://www.ansys.com/products/fluids/ansys-fluent
[21] © ANSYS rights reserved. Ansys Fluent 12.0 Theory Guide - 1.2 Continuity and Momentum Equations. [cited 2024 Feb 1]. Available from: https://www.afs.enea.it/project/neptu-nius/docs/fluent/html/th/node11.html
[22] Alfonsi G. Reynolds-averaged Navier-Stokes equations for turbulence modeling. Appl Mech Rev. 2009;62(4):1–20.
[23] J SSJ. Quality Systems Group. ITTC (n.d) ITTC-Recommended Proced Guidel ITTC Qual Syst Man Recomm Proced Guidel. 2013;
[24] Carlton J. Marine Propellers and Propulsion 4th Edition. Vol. 0, Marine Propellers and Propulsion. 2018. 0
[25] Gatski TB, Speziale CG. On Explicit Algebraic Stress Models for Complex Turbulent Flows. J Fluid Mech. 1993;254:59–78.
[26] Gao Q, Jin W, Vassalos D. The calculations of propeller induced velocity by RANS and momentum theory. J Mar Sci Appl. 2012;11(2):164–8.